Experimental analysis of the cavitating flow induced by an ultrasonic horn

Saskia Müller[1], Maurice Fischper[1], Stephan Mottyll[1], Romuald Skoda[1] and Jeanette Hussong[1]

[1] *Ruhr Universität Bochum, chair of hydraulic fluid machinery, Germany, saskia.s.mueller@rub.de*

Introduction

To generate an empirical relation between cavitation intensity and various experimental conditions the frequency distribution of ultrasound induced cavitation bubbles is investigated experimentally. For this a self-developed image processing algorithm was used for analyzing the time averaged statistical relation between bubble size and number.

It is well known that cavitation occurring close to surfaces will cause damage of components. The degree of damage strongly depends on a variety of influencing factors such as pressure, temperature etc. For principle examination an ultrasonic horn, the sonotrode, is often used to study cavitation erosion [1]. According to the acoustic intensity, which changes with the actuation amplitude, cavitation bubble figures will change [2]. In the past bubble dynamics and oscillation behavior of single cavitation bubbles were investigated [3]. However, ultrasound induced multi bubble systems show a nonlinear dynamical response behavior that is understood only partially till today [4, 5]. Although cavitation bubbles were detected and classified into groups [6], statistical analysis of a bubble size distribution was done only in a small scale experiment till today [7]. The present study aims to elaborate a time averaged statistical relation between the number and size distribution of cavitation bubbles in large bubble systems created by an ultrasonic horn, hence on referred to as "bubble spectrum". The postprocessing procedure developed is applicable to a broad range of experimental conditions.

Experimental set up

The experimental set up used for analyzing the bubble spectrum consists of an ultrasonic horn (sonotrode, Hielscher GmbH) with a triggering unit, an octogonal water beaker for good optical access and a shadowgraphy imaging system (see figure 1). The sonotrode is a dynamic oscillator with a working frequency of approximately 20 kHz and an adjustable peak to peak Amplitude (A_{pp}) covering a range of 20-50 µm. Recordings of the cavitation bubbles are obtained with a shadowgraphy imaging system, which includes a Nd :YAG dual cavity laser (Quantel, Evergreen) for illumination, a double frame CCD-camera (ImagerProSX 5M, LaVision) and an optical diffusion light unit to achieve a homogeneous scattered illumination. Deionized water was chosen as working fluid for the experiments. The cylindrically shaped sonotrode tip is positioned on the centerline axis of the beaker and reaches 5 mm deep into the water.

The pulsed dual cavity laser serves as light source providing exposure times of 6 ns. With a chosen field of view (FOV) of 22.13 x 18.27 mm², an optical resolution of 8.91 µm per pixel is reached. Recordings are taken on the vertical xy-center plane below the sonotrode as illustrated in figure 1. The measurement sequences are synchronized with the actuation phase of the sonotrode, so phase locked images throughout the actuation phase are taken. For each measurement 200 pictures were taken for evaluation with the algorithm.

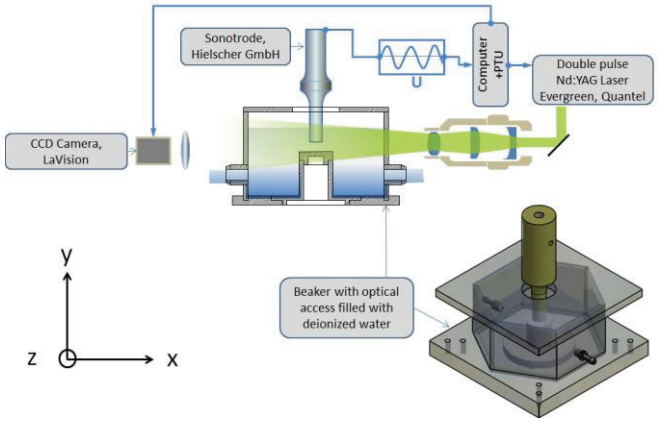

Figure 1: Test set up for measuring the bubble spectrum.

Image processing algorithm

For analyzing the cavitation bubble spectrum a self-developed MATLAB algorithm is used. Firstly, to ensure a consistent image background intensity the time averaged background intensity before actuation is subtracted from each examined recording.

Secondly, intensity gradients of the image are calculated in both, horizontal and vertical direction and hence on the Euclidean norm are calculated ($z = \sqrt{x^2 + y^2}$). High gradient values are associated with potential edges of an object. To determine whether a pixel belongs to an edge or not a threshold is used on the gradient image. Due to spatial bubble concentration gradients throughout the FOV differences in image contrast, that is bubble to background intensity ratios, occur. Therefore, the image is divided into two areas in which different values for the intensity gradient thresholds are depicted which will be optimized in a later stage of the evaluation procedure.

Implementing the gradient threshold to find edges of a detected object results in a binary image ("1" for pixels that are part of an object, "0" for those who are not). The detected areas are represented by their boundary and the interior of an object is filled with a binary "1" if the boundary is a closed object.

Afterwards the object properties of each detected item are inspected to fulfill certain criteria before the detected object is interpreted as a single bubble, entering the statistical evaluation procedure hence on. The criteria are as follows:

- the nominal bubble image diameter must be minimal four pixels
- the average intensity of a detected object must be less than 60 % of the maximal intensity counts
- the eccentricity of an object must be smaller than 0.9

The remaining objects are classified as bubbles. Before the final statistical evaluation, two parameters were optimized with a double loop MATLAB routine to determine the thresholds for which a maximum amount of cavitation bubbles can be detected: the intensity threshold for dividing the image into two searching areas and the intensity gradient thresholds for the bubble edge detection.

Results

The result of the optimization loop is shown in figure 2. Curves indicate the amount of detected cavitation bubbles as function of the chosen gradient intensity threshold in two optimized searching areas of low (blue) and high (red) bubble density, respectively. As can be seen a maximum forms in both searching areas. On the one hand an increasing threshold of the intensity gradient defocused cavitation bubbles or bubbles of lower intensity contrast to the background are more easily deselected. On the other hand if the threshold falls below a certain value individual, neighboring cavitation bubbles might be detected as one entity which hence on is deselected based on the eccentricity criterion.

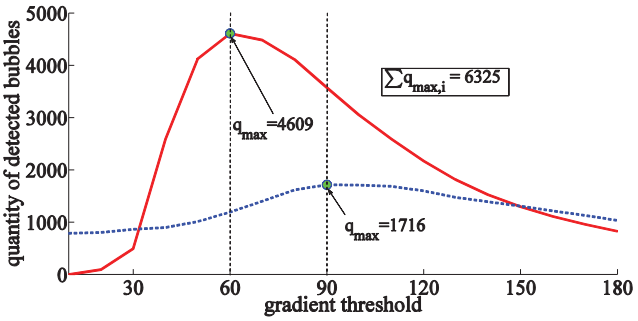

Figure 2: Intensity study to select a gradient threshold to achieve a maximum amount of bubbles

Based on the probability density function the separation of the images into two searching areas was done. Figure 3a shows a snapshot of the cavitation region. The corresponding locations of detected single cavitation bubbles are shown in figure 3b marked with red dots.

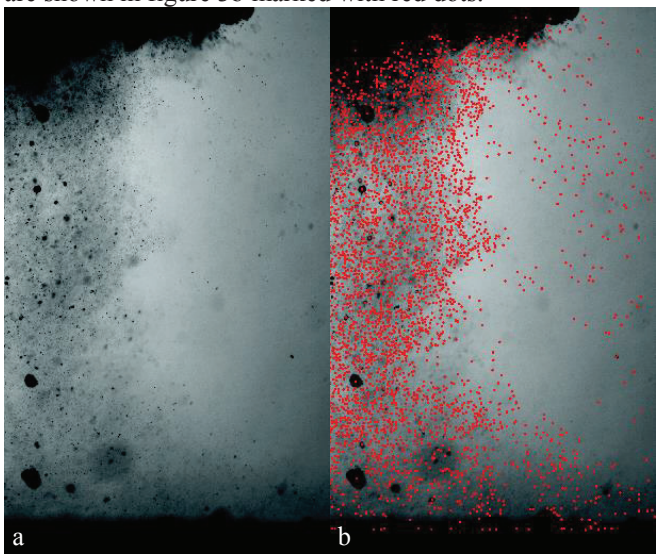

Figure 3: a) snapshot of the bubbles spectrum under the sonotrode tip b) marked bubbles detected by the algorithm

A representative result of the statistical analysis is given by figure 5. Probability density functions of detected cavitation bubbles are plotted as function of the bubble radius for two different actuation amplitudes A_{pp}=50 µm and A_{pp}=20 µm. As would be expected, the bubble spectrum scales with the input power [5], maintaining a characteristic exponential decrease in number density with growing bubble size.

Conclusion

The self-developed algorithm presented here was optimized to detect the maximum amount of cavitation bubbles beneath the sonotrode for a wide range of experimental conditions. The optimization procedure includes a threshold search in terms of intensity and gradient intensity values.
A qualitative comparison of the frequency distribution with results derived from Rivas et al. [7] and others shows that the exponential decrease as it is evident in figure 4 seems to be a characteristic, scale invariant feature of both small and large bubble systems that may cover a few hundred up to several thousand individual bubbles likewise.

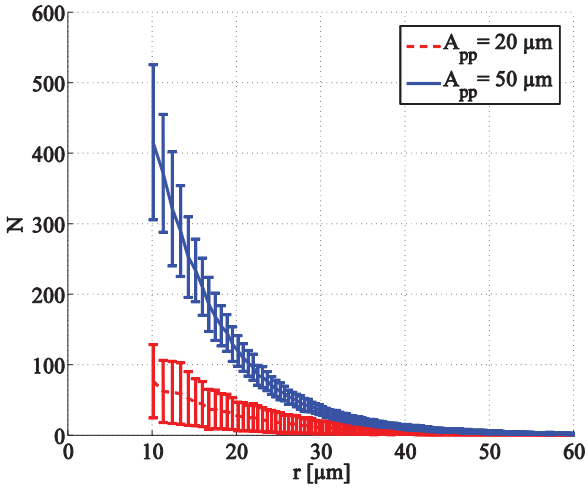

Figure 4: Bubble spectrum at A_{pp} 50 µm and A_{pp} 20 µm

References

[1] A. Jayaprakesh, J.-K. Choi, G. L. Chahine, F. Martin, M. Donnelly, J.-P. Franc, Wear, **296**, (2012), 619-629

[2] A. Moussatov, R. Mettin, C. Granger, T. Tervo, B. Dubus, W. Lauterborn, WCU, Paris (2003), 955-958

[3] R. Mettin, T. Nowak, DAG/DAGA, Rotterdam (2009)

[4] M. Dular, R. Mettin, A. Žnidarčič, V. A. Truon, CAV12, Singapore (2012), 741-745

[5] R. Mettin, Oscillations, Waves and Interactions, Universitätsverlag Göttingen (2007), 171-198

[6] T. Nowak, R. Mettin, W. Lauterborn, DAG/DAGA, Rotterdam (2009)

[7] D. F. Rivas, L. Stricker, A. G. Zijlstra, H. J. G. E. Gardeniers, D. Lohse, A. Prosperetti, Ultrasonics Sonochemistry, **20**, (2013), 510-524